Sonodynamic effect based on vancomycin-loaded microbubbles or meropenem-loaded microbubbles enhances elimination of different biofilms and bactericidal efficacy

From First Affiliated Hospital of Xinjiang Medical University, Urumqi, China

Cite this article:
Bone Joint Res 2024;13(9):
441–451.

DOI: 10.1302/2046-3758.
139.BJR-2023-0319.R3

Correspondence should be sent to Wenbo Mu
498287267@qq.com

L. Yao,[1] C. Chu,[2] Y. Li,[3] L. Cao,[3,4] J. Yang,[5] W. Mu[3,5]

[1]Department of Sports Medicine, First Affiliated Hospital of Xinjiang Medical University, Urumqi, China
[2]Department of Joint Surgery, First Affiliated Hospital of Sun Yat-sen University, Guangzhou, China
[3]Department of Orthopaedics, First Affiliated Hospital of Xinjiang Medical University, Urumqi, China
[4]Key Laboratory of High Incidence Disease Research in Xinjiang (Xinjiang Medical University), Ministry of Education, Urumqi, China
[5]College of Pharmacy, Xinjiang Medical University, Urumqi, China

Aims

This study investigated vancomycin-microbubbles (Vm-MBs) and meropenem (Mp)-MBs with ultrasound-targeted microbubble destruction (UTMD) to disrupt biofilms and improve bactericidal efficiency, providing a new and promising strategy for the treatment of device-related infections (DRIs).

Methods

A film hydration method was used to prepare Vm-MBs and Mp-MBs and examine their characterization. Biofilms of methicillin-resistant *Staphylococcus aureus* (MRSA) and *Escherichia coli* were treated with different groups. Biofilm biomass differences were determined by staining. Thickness and bacterial viability were observed with confocal laser scanning microscope (CLSM). Colony counts were determined by plate-counting. Scanning electron microscopy (SEM) observed bacterial morphology.

Results

The Vm-MBs and Mp-MBs met the experimental requirements. The biofilm biomass in the Vm, Vm-MBs, UTMD, and Vm-MBs + UTMD groups was significantly lower than in the control group. MRSA and *E. coli* biofilms were most notably damaged in the Vm-MBs + UTMD group and Mp-MBs + UTMD group, respectively, with mean 21.55% (SD 0.08) and 19.73% (SD 1.25) remaining in the biofilm biomass. Vm-MBs + UTMD significantly reduced biofilm thickness and bacterial viability ($p = 0.005$ and $p < 0.0001$, respectively).

Mp-MBs + UTMD could significantly decrease biofilm thickness and bacterial viability (allp < 0.001). Plate-counting method showed that the numbers of MRSA and *E. coli* bacterial colonies were significantly lower in the Vm-MBs + UTMD group and the Mp, Mp-MBs, UTMD, Mp-MBs + UTMD groups compared to the control group ($p = 0.031$). SEM showed that the morphology and structure of MRSA and *E. coli* were significantly damaged in the Vm-MBs + UTMD and Mp-MBs + UTMD groups.

Conclusion

Vm-MBs or Mp-MBs combined with UTMD can effectively disrupt biofilms and protectively release antibiotics under ultrasound mediation, significantly reducing bacterial viability and improving the bactericidal effect of antibiotics.

Bone & Joint Research

Article focus

- The effect of combining ultrasound-targeted microbubble destruction (UTMD) with vancomycin-microbubbles (Vm-MBs) and meropenem (Mp)-MBs treatment on the elimination of methicillin-resistant *Staphylococcus aureus* (MRSA) and *Escherichia coli* biofilms and the improvement of bactericidal efficiency, thus providing a strategy of treatment of device-related infections (DRIs).

Key messages

- Vm-MBs or Mp-MBs can penetrate biofilms, enhancing the effect of drug entry into deeper layers of the biofilm.
- When combined with UTMD, the structure of the biofilms can be destroyed, allowing for the release of drugs and improving bactericidal efficiency.

Strengths and limitations

- The study developed a novel way for antibiotic-loaded MBs to penetrate biofilms, enhancing the opportunities for drug entry into deeper layers of the biofilms and destroying biofilms in combination with the UTMD technique, which is of great importance to provide an experimental basis for the treatment of biofilm-related infections.
- It is noted that antibiotic penetration of biofilm is time-dependent. A limitation of this study is the lack of investigation into the time-based relationship between antibiotic and drug-loaded MB penetration.
- The study lacked in vivo experiments, control group with MBs without antibiotics, and mechanism exploration of antibiotic-loaded MBs + UTMD technique treatment for biofilm.

Introduction

In recent years, with the growing popularity of medical devices and implants, the rate of device-related infections (DRIs) has continuously increased. The number of patients with periprosthetic joint infection (PJI) is expected to increase to 250,000 per year by 2030 in the USA.[1] The increasing number of open fractures in older patients also adds to the risk of fracture-related infection (FRI), which occurs in 4% to 52% of Gustilo-Anderson grade III fractures with soft-tissue damage.[2] Meanwhile, the incidence rate of implant-associated spinal infection is as high as 10%.[3] Treatment of DRIs usually requires several rounds of surgery, further increasing the financial burden and chance of fatality postoperatively.[4,5] Some studies have indicated that biofilms are considered to be the main reason for the occurrence of DRIs and the development of chronic infections.[6-8]

Biofilms are an aggregative form of microbial life which tend to adhere to interfaces of prostheses or internal fixation devices, owing to the presence of extracellular polymeric substances (EPS) on biofilms.[9] On the one hand, biofilms on prostheses protect bacteria from surrounding environmental stresses, impede antibiotic penetration, and confer long-term persistence capacity.[10,11] On the other hand, biofilms cause antibiotic inactivation by degradation or absorption to EPS.[12] Therefore, it is hard to cure DRIs by using traditional antibiotic therapy.[13,14] A therapeutic strategy, either as an adjunct to directly break up biofilms or enhance antibiotic efficacy, would be a significant breakthrough for DRI treatment.

Some researchers have proposed that physical methods will become a potential method to destroy biofilm structure and then improve sterilization efficacy.[15,16] Tahir et al[17] made use of silver substitution of cobalt ferrite under laser stimulation, which has an optimal sterilization effect. However, the uptake of Ag+ in this method damages cells. Meanwhile, research has indicated that photodynamic therapy has certain limitations, including the phototoxicity of the photosensitizer and the efficacy of photodynamic therapy, which is related to irradiation depth.[18] Light can only be irradiated to 2 to 3 μm below the skin's surface, meaning that it only has a therapeutic effect on superficial bacteria.

Sonodynamic therapy makes up for the shortcomings of photodynamic therapy. First, it can reach deep into the tissue and exert a bactericidal effect. Moreover, it is safer, owing to the harmlessness of the clinical contrast agent known as microbubbles (MBs) as a medium compared with photodynamic therapy. Under the effect of ultrasound (US), MBs can contract oscillatory (continuous changes in

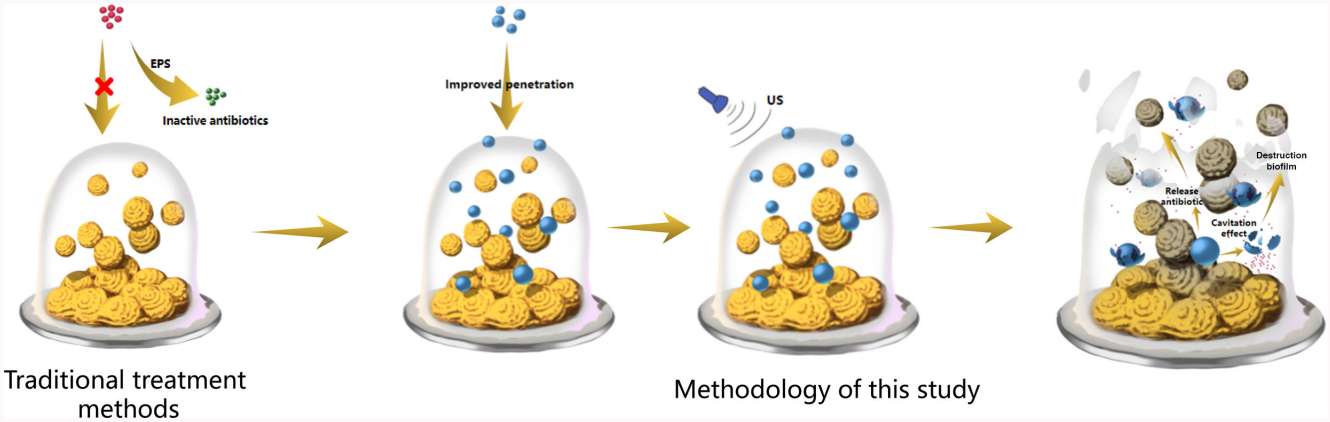

Fig. 1

Schematic illustration of the difference between this study's treatment method and conventional treatment methods, and the mechanism of ultrasound-targeted microbubble destruction (UTMD) combined with vancomycin-microbubbles (Vm-MBs) and meropenem (Mp)-MBs to exert cavitation effect. EPS, extracellular polymeric substances; US, ultrasound.

Table I. Experimental interventions.

Group	Intervention
MRSA	
Control	Saline
Vm	Vm diluted with saline to concentration of 32 μg/ml
Vm-MBs	Vm-MBs diluted with saline to concentration of 10^6 pieces/ml
UTMD	MBs with 10^6 pieces/ml combined with US
Vm-MBs + UTMD	Vm-MBs with 10^6 pieces/ml combined with US
E. coli	
Control	Saline
Mp	Mp diluted with saline to concentration of 16 μg/ml
Mp-MBs	Mp-MBs diluted with saline to concentration of 10^6 pieces/ml
UTMD	MBs with 10^6 pieces/ml combined with US
Mp-MBs + UTMD	Mp-MBs with 10^6 pieces/ml combined with US

MB, microbubble; Mp, meropenem; MRSA, methicillin-resistant *Staphylococcus aureus*; US, ultrasound; UTMD, ultrasound-targeted microbubble destruction; Vm, vancomycin.

microbubble pressure are induced by ultrasound, which dynamically responds to pressure changes by contraction and expansion; when excited with sufficient amplitude, the bubble radius and external pressure are inhomogeneous, suggesting that the bubbles may rebound upon collapse or exhibit expansion or complete implosion, which is known as the cavitation effect), and generate local microstreams by inertial cavitation to disrupt the integrity of cell membranes near MBs, thus increasing the dose of drugs reaching specific sites and their efficacy.[19] The exerting sonodynamic effect was also used as the theoretical basis of ultrasound-targeted microbubble destruction technology (UTMD). So far, the application of UTMD in anti-infection treatment is still in its infancy. Therefore, we selected methicillin-resistant *Staphylococcus aureus* (MRSA) and *Escherichia coli,* which are often used in biofilm experiments. Then, considering the high efficacy of vancomycin (Vm) and meropenem (Mp) on treating Gram-positive and Gram-negative infection,[20,21] we designed Vm-MBs and Mp-MBs to interfere with biofilms of the two bacteria species. We performed the study to determine the effect of Vm-MBs and Mp-MBs combined with UTMD on the disruption of different bacterial biofilms and the protective release of antibiotics to improve the antibiotics' bactericidal effect, in order to provide some insight into the efficacy of sonodynamic therapy in treating biofilm-associated infections (Figure 1).

Methods

Vm-MB and Mp-MB preparation and characterization

The Vm-MBs and Mp-MBs were prepared using the thin-film hydration method.[22] Briefly, 1,2-distearoyl-sn-glycero-3-phosphocholine (DSPC) and 1,2-distearoyl-sn-glycero-3-phosphoethanolamine-N-[methoxy(polyethylene glycol)-2000] (DSPE-PEG2000), in a molar ratio of 9:1, were dissolved in chloroform together with 20 μl Vm stock solution and 20 μl Mp stock solution (1 mg Vm and 1 mg Mp dissolved in 20 μl saline). The solvent was evaporated using a steady stream of nitrogen and dried under a vacuum for over three hours. The resulting lipid film was reconstituted by suspending it in a solution containing glycerol, propylene glycol, and 0.1 M Tris-buffered saline (TBS, pH 7.4) in a ratio of 10:10:80 (v/v/v), at a temperature of 65°C. The lipid solution was then subpackaged into vials (1 ml per vial). After sealing the cap, the gas was replaced with perfluoropropane gas (C_3F_8) in vials. Subsequently, the vial was shaken mechanically for 30 seconds using an agitator. 'Empty' MBs were made using the same method as above, without adding antibiotics during the preparation process.

The morphologies of MBs, Vm-MBs, and Mp-MBs were observed by confocal laser scanning microscope (CLSM) (Leica, Germany). A zeta potential analyzer (Brookhaven Instruments, USA) calculated the size, zeta potential, and polydispersity index (PDI) of MBs, Vm-MBs, and Mp-MBs. The content of Vm and Mp loaded in MBs was calculated using high-performance liquid chromatography (HPLC) (Agilent, USA). Drug encapsulation and drug loading efficiencies were calculated using the following formulae: Drug encapsulation efficiency (%) = weight of antibiotics in MBs/weight of the total amount of antibiotics in the preparation of MBs × 100%; Drug loading efficiency (%) = weight of antibiotics in MBs/weight of total antibiotics-loaded MBs × 100%.

Storage time may result in changes in drug loading and encapsulation efficiencies. The Vm-MBs and Mp-MBs were stored in small glass vials at 4°C for one, three, five, 12, and 24 hours, respectively, and periodically centrifuged. The collected solution was used to estimate the amount of Vm and Mp leakage by HPLC. The percentage of leakage of Vm(%) = weight of leakage of Vm/weight of Vm in MBs × 100%. The percentage of leakage of Mp was the same as Vm.

Cultivation of bacteria and biofilm formation

MRSA (USA300) and *E. coli* (ATCC25922) were inoculated in 5 ml tryptic soy broth (TSB) + 0.5% dextrose (Solarbio Science & Technology, China), and allowed to grow overnight at 37°C with agitation (180 rpm/min). The bacteria were harvested and resuspended in TSB + 0.5% dextrose at a turbidity of 0.5 McFarland. MRSA and *E. coli* biofilms were developed in six-well plates, confocal dishes, and cell-climbing tablets (LabServ; Thermo Fisher Scientific, USA). Bacteria suspension (2 ml) at 0.5 McFarland was added into six-well plates, confocal dishes, and cell-climbing tablets incubated at 37°C for 24 hours. Bacteria adhered to the bottom and formed biofilms.

Minimum inhibitory concentration and minimum bactericidal concentration

The antimicrobial effect of Vm and Mp was assessed using a serial two-fold dilution technique. Vm and Mp were first

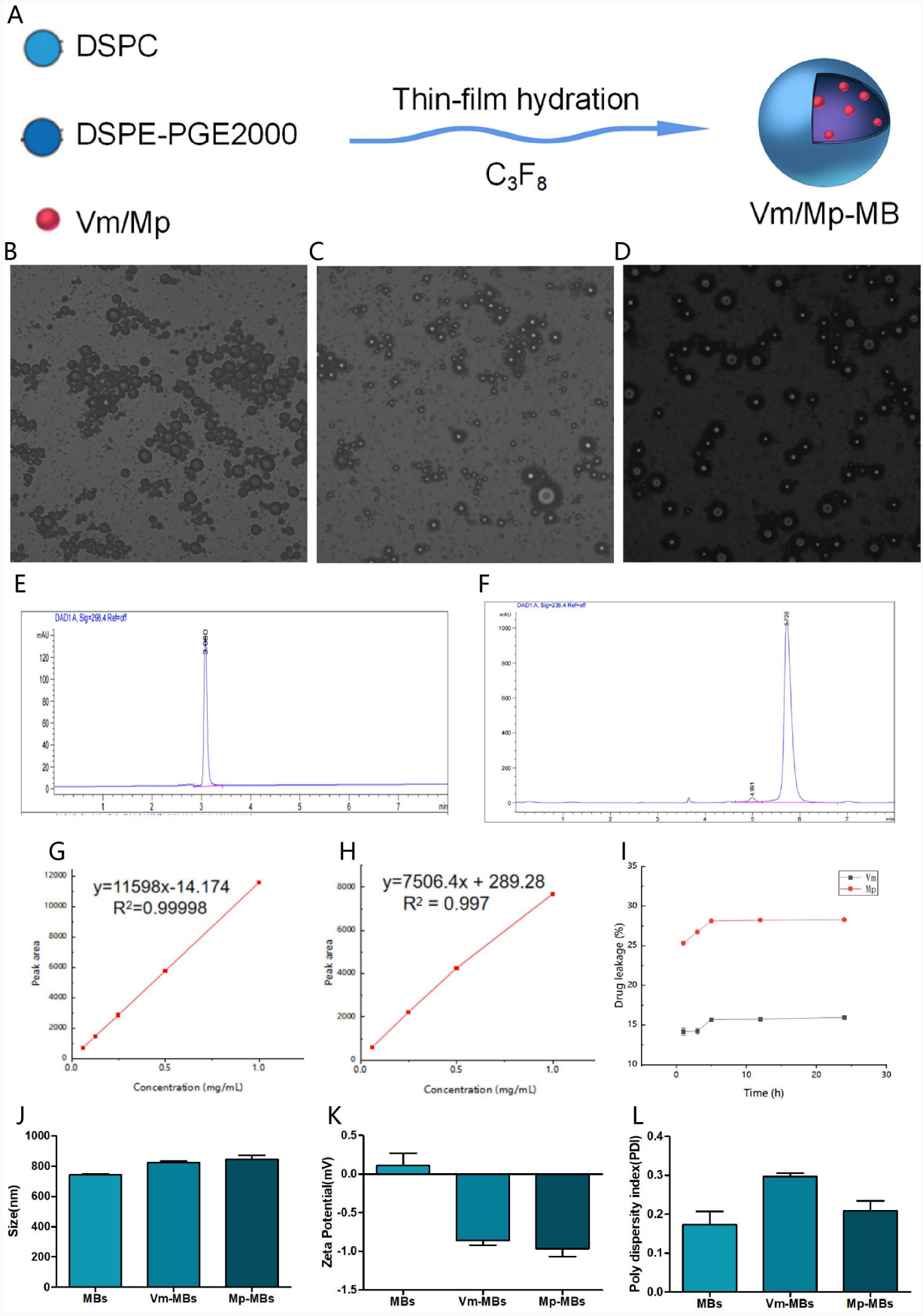

Fig. 2

Characterization of vancomycin (Vm)/meropenem-microbubbles (Mp-MBs). a) Schematic illustration of the preparation of Vm/Mp-MBs. b) to d) Confocal laser scanning microscope (CLSM) images of blank MBs, Vm-MBs, and Mp-MBs (200×). e) Vancomycin (Vm) high-performance liquid chromatogram (HPLC). f) Meropenem HPLC. g) Vm concentration versus peak area standard curve. h) Meropenem (MP) concentration versus peak area standard curve. i) Drug leakage of Vm or Mp from Vm-MBs or Mp-MBs into phosphate-buffered saline (PBS) at 4°C at different timepoints. j) Size of blank MBs, Vm-MBs, and Mp-MBs. k) Zeta potential of blank MBs, Vm-MBs, and Mp-MBs. l) Polydispersity index of blank MBs, Vm-MBs, and Mp-MBs. DSPC, 1,2-distearoyl-sn-glycero-3-phosphocholine; DSPE-PGE2000, 1,2-distearoyl-sn-glycero-3-phosphoethanolamine-N-[methoxy(polyethylene glycol)-2000].

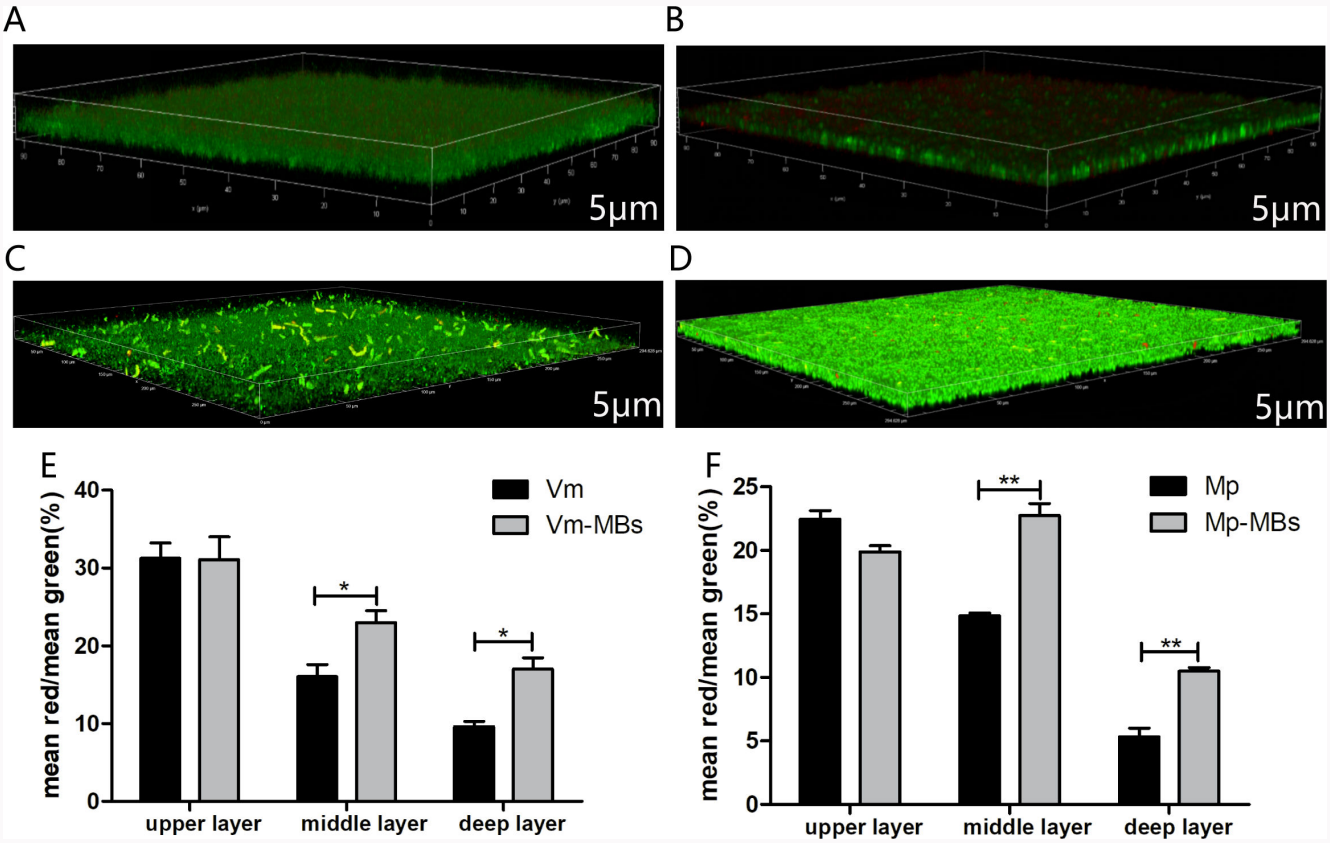

Fig. 3

Vancomycin (Vm), Vm-microbubble (MB), meropenem (Mp), and Mp-MB penetration through biofilms. a) to d) 3D confocal images of different bacterial biofilms (green) and Vm, Vm-MBs, Mp, and Mp-MBs (all red). a) Confocal image of Vm penetration through methicillin-resistant *Staphylococcus aureus* (MRSA) biofilms. b) Confocal image of Vm-MB penetration through MRSA biofilms. c) Confocal image of Mp penetration through *Escherichia coli* biofilms. d) Confocal images of Mp-MB penetration through *E. coli* biofilms. e) Comparison of Vm and Vm-MB concentration in different layers through detection of the fluorescence intensity in the upper, middle, and deep layers. f) Comparison of Mp and Mp-MB concentration in different layers through detecting the fluorescence intensity in the upper, middle, and deep layers. The results are presented as mean and SD (n = 3), and p-values were calculated using independent-samples *t*-test. *p < 0.05; **p < 0.01; ***p < 0.001.

diluted in Mueller Hinton Broth (MHB). Successive two-fold dilutions of Vm and Mp were made to achieve concentrations ranging from 0.5 to 32 μg/ml. The determination of minimum inhibitory concentration (MIC) and minimum bactericidal concentration (MBC) for Vm and Mp followed the method outlined by Kot et al.[23]

Vm, Vm-MB, Mp, and Mp-MB penetration through biofilms

After 24 hours of growth, the biofilms were treated with 20 μmol/l SYTO9 dye (Thermo Fisher Scientific) for 15 minutes at room temperature to ensure complete penetration and shield from light. Subsequently, they were rinsed three times with double-distilled water to remove the supernatant. Vm, Mp at a concentration of 32 μg/ml (Cy5-labelled) (Rui Xi Biotechnology, China), Vm-MBs, and Mp-MBs at a concentration of 10^6 pieces/ml were stained with Dil (Ruitaibio, China), and then incubated with SYTO9-labelled biofilms for 15 minutes in a dark room. Following this, the supernatant was removed, and the biofilms were washed with 1 ml double-distilled water to eliminate excess Vm, Mp, Vm-MBs, and Mp-MBs. To assess the ability of the two antibiotics and two antibiotics-MBs to penetrate the biofilms, we examined their distribution within the biofilms using CLSM. SYTO9 was excited at 480/500 nm, Dil used the 549 nm laser line, and Cy5 was excited at 650/670 nm.

Experimental ultrasound-targeted microbubble destruction protocol

For the MRSA, the experiment was divided into a control group, Vm group, Vm-MBs group, UTMD group, and Vm-MBs + UTMD group. For the *E. coli*, the experiment was divided into a control group, Mp group, Mp-MBs group, UTMD group, and Mp-MBs + UTMD group. Vm and Mp were diluted with saline to a final concentration of 32 μg/ml.[19,24] Vm-MBs and Mp-MBs were diluted with saline to a final concentration of 10^6 pieces/ml.[25] Ultrasonic parameters: frequency was 1.7 to 3.4 MHz, mechanical index (MI) was 0.6, and duration of stimulation was two minutes.[26] Later, the bacteria suspension that grew for 24 hours was removed, and planktonic bacteria were washed out. Then, for the MRSA, saline was added to the control group, and corresponding concentrations of Vm, Vm-MBs were added to the other four groups. The Vm-MBs + UTMD and UTMD groups were intervened by ultrasound under specified ultrasonic parameters. The experimental process of *E. coli* was the same as MRSA (Table I).

Biofilm elimination and bactericidal efficacy

Biofilm biomass was quantified using the quantitative crystalline violet staining method. First, the supernatant of the biofilm was removed and washed by phosphate-buffered saline (PBS) three times. Next, biofilm was fixed with

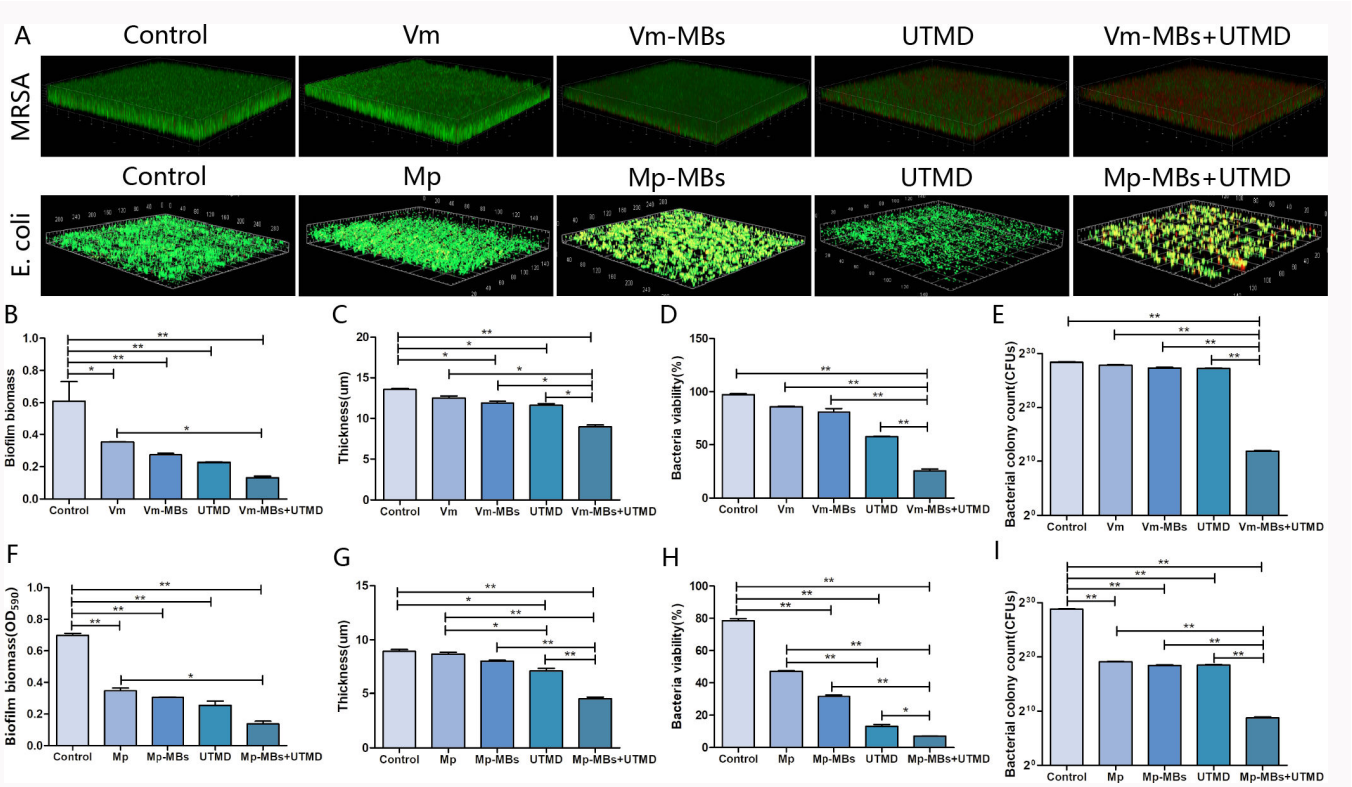

Fig. 4

Treatment of methicillin-resistant *Staphylococcus aureus* (MRSA) and *Escherichia coli* biofilms with vancomycin-microbubbles (Vm-MBs) or meropenem (Mp)-MBs + ultrasound-targeted microbubble destruction (UTMD) in vitro. a) 3D confocal laser scanning microscope (CLSM) images of MRSA and *E. coli* biofilms stained with LIVE/DEAD after treatment. b) and f) Crystal violet-stained MRSA and *E. coli* biofilm biomass after various treatments (n = 3, means and SD). c) and g) Relative MRSA and *E. coli* biofilm thickness after various treatments. d) and h) Relative MRSA and *E. coli* biofilm bacterial viability after various treatments. e) and i) Relative MRSA and *E. coli* bacterial colony counts after various treatments. j) Relative standard plate-counting method of MRSA and *E. coli* biofilms after various treatments. k) Scanning electron microscopy (SEM) images of MRSA and *E. coli* biofilms after various treatments (10,000x). The results are presented as mean and SD (n = 3). All the results were calculated using independent-samples *t*-test. *p < 0.05; **p < 0.01.

100% methanol for 15 minutes before removing the methanol. The residual methanol was evaporated at 37°C for ten minutes, followed by staining with 1% crystal violet solution for eight minutes before removal. The supernatant was washed with running water until colourless to get rid of the residual unbound crystal violet, and 10% acetic acid was added. Finally, the optical density (OD) value was read using the enzyme-labelled plate (DeTie, China) absorbance meter at a wavelength of 570 nm. After undergoing experimental intervention, the biofilms were stained with LIVE/DEAD (Thermo Fisher Scientific) for 15 minutes and protected from light after various treatments, and the morphology and thickness of the biofilms, as well as the viability of the bacteria inside the biofilm, were observed by CLSM. Meanwhile, the colony-forming units (CFUs) of viable biofilm bacteria was analyzed using the standard plate-counting method.[27] Bacteria were grown on the surface of cell climbing tablets to show the morphology of bacteria cells. After various treatments, the tablets were fixed with glutaraldehyde solution (2.5%) for four hours and then sequentially dehydrated with series concentrations of ethanol solutions (50%, 70%, 80%, 90%, and 100%) for 15 minutes. The morphology of bacteria was obtained by scanning electron microscopy (SEM) (Leica) after being coated with gold.

Statistical analysis

SPSS Statistics 25 (IBM, USA) was used to analyze the data. The Shapiro-Wilk test was used to test the normality of the datasets. One-way analysis of variance and independent-samples *t*-test were used for normally distributed data. The Kruskal-Wallis and Mann-Whitney U tests were used for non-normally distributed data. Differences with a p-value < 0.05 were considered statistically significant.

Results

Characterization of Vm-MBs and Mp-MBs

The Vm-MBs and Mp-MBs were prepared by the thin film hydration method, where C_3F_8 gas and Vm or Mp solution were filled inside MBs (Figure 2a). CLSM images (Figure 2b to 2d) showed that the blank MBs, Vm-MBs, and Mp-MBs exhibited spherical shapes and were well dispersed. The initial dose of 1.0 mg Vm and Mp was used to prepare the Vm-MBs and Mp-MBs, respectively. The mean drug encapsulation efficiency of Vm-MBs and Mp-MBs was 84.66% (SD 0.38) for Vm and 74.70% (SD 0.45) for Mp. The mean drug loading efficiency was 27.13% (SD 0.24) for Vm and 23.94% (SD 0.15) for Mp (Figure 2e to 2h). When stored at 4°C, the mean drug leakage from Vm-MBs and Mp-MBs after 24 hours was measured to be 15.93% (SD 0.03) for Vm and 28.27% (SD 0.26) for Mp (Figure 2i). The mean size, zeta potential, and PDI of the

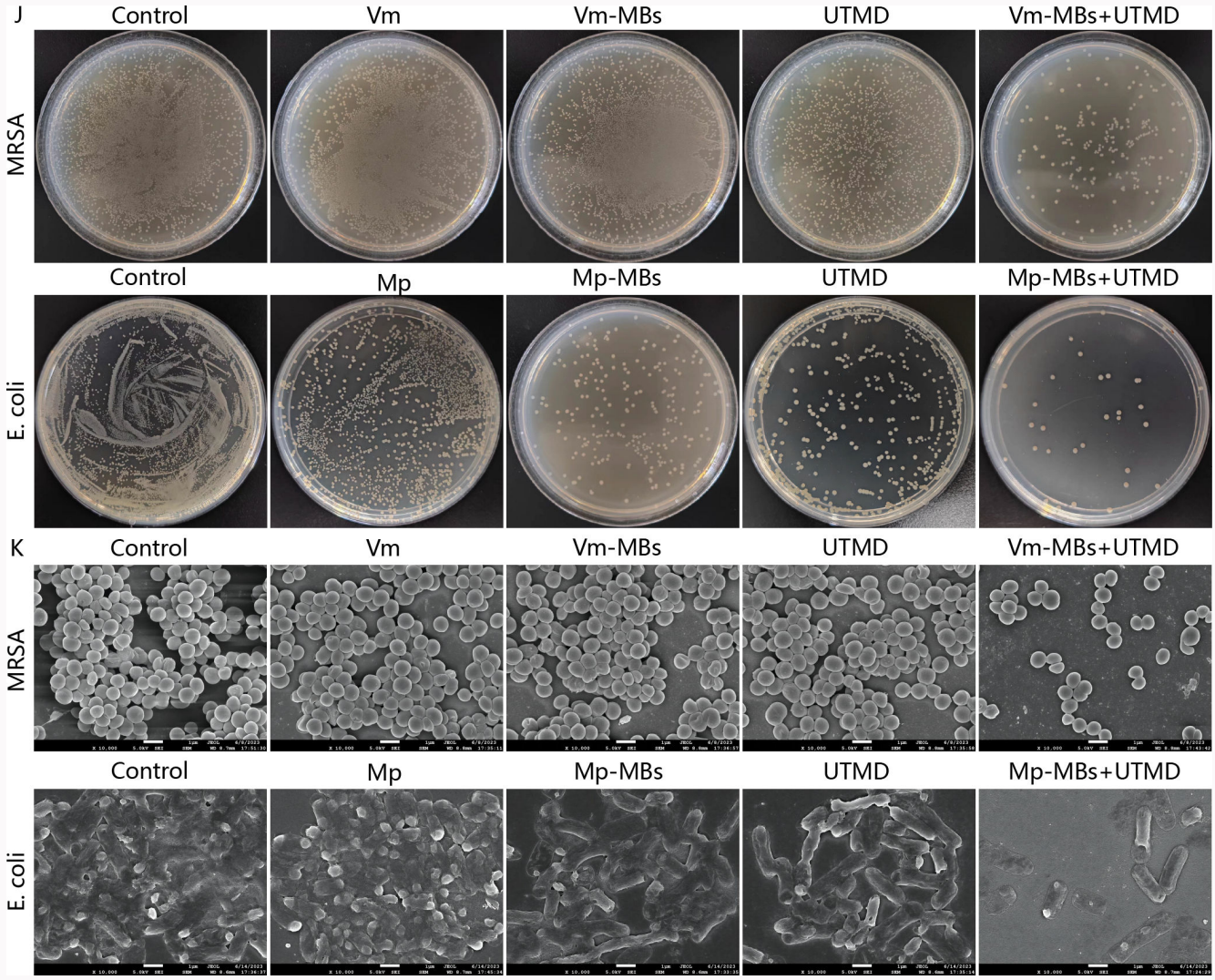

Fig. 5
Treatment of methicillin-resistant *Staphylococcus aureus* (MRSA) and *Escherichia coli* biofilms with vancomycin-microbubbles (Vm-MBs) or meropenem (Mp)-MBs + ultrasound-targeted microbubble destruction (UTMD) in vitro. a) Relative standard plate-counting method of MRSA and *E. coli* biofilms after various treatments. b) Scanning electron microscopy (SEM) images of MRSA and *E. coli* biofilms after various treatments (10,000×). The results are presented as mean and SD (n = 3).

blank MBs, Vm-MBs, and Mp-MBs are summarized in Figure 2j to 2l.

Antimicrobial susceptibility results of planktonic bacteria

We tested the MIC and MBC of planktonic MRSA bacteria to Vm and planktonic *E. coli* bacteria to Mp. The results indicated that the MIC and MBC values for MRSA were 2 μg/ml and 8 μg/ml, respectively, while the MIC and MBC values for *E. coli* were 0.015625 μg/ml and 0.0625 μg/ml, respectively.

Vm, Vm-MB, Mp, and Mp-MB penetration through biofilms

Gram-positive bacteria MRSA and Gram-negative bacteria *E. coli* were chosen as models to investigate Vm, Vm-MBs, Mp, and Mp-MBs that could penetrate biofilms. 3D CLSM images confirmed that Vm appeared to bind only to the surface of the biofilms, with bacteria within the deepest layers exhibiting minimal red fluorescence (Figure 3a). In contrast, upon addition of Vm-MBs to the biofilm, deeper layers became fluorescent (Figure 3b). Compared with Vm alone, Vm-MBs showed significantly greater penetration into the deeper layers of the biofilm ($p = 0.014$, independent-samples *t*-test) (Figure 3e). A similar result could be observed using *E. coli* as the experimental model ($p < 0.01$, independent-samples *t*-test) (Figures 3c, 3d, and 3f).

Evaluation of biofilm elimination and bactericidal efficacy against biofilm bacteria

The elimination of biofilms was confirmed through crystalline violet staining and CLSM. 3D CLSM images demonstrated that dense and packed biofilms were observed in the control group. The structures of MRSA biofilms in Vm and Vm-MBs groups exhibited limited changes. In contrast, loosened structure and many micropores were observed after treatment in the UTMD or Vm-MBs + UTMD groups. The same results were demonstrated in *E. coli* biofilms (Figure 4a). The results of MRSA biofilm crystal violet staining showed statistically significant differences in the biofilm biomass of the Vm, Vm-MBs, UTMD, and Vm-MBs + UTMD groups as compared to that of the control group (results were expressed as mean ± SD (N = 3), $p = 0.002$, 0.009, 0.007, and < 0.0001, respectively,

and were calculated using the Student's t-test calculation. *P < 0.05; **P < 0.01; ***P < 0.001).

Meanwhile, the MRSA biofilm was more notably damaged, with approximately mean 21.55% (SD 0.08) remaining in biofilm biomass in the Vm-MBs + UTMD group (Figure 4b). The *E. coli* biofilm was destroyed, with approximately mean 19.73% (SD 1.25) remaining in biofilm biomass in the Mp-MBs + UTMD group (Figure 4f). A more noticeable decrease in mean biofilm thickness (9.6 μm (SD 1.56)) was found in the Vm-MBs + UTMD group (Figure 4c). A significant decrease in mean biofilm thickness was found in the Mp-MBs + UTMD group (4.5 μm (SD 0.3)) (Figure 4g). On CLSM images, green fluorescence represents viable cells, whereas red fluorescence represents dead cells. As indicated in Figure 4d, significantly more dead bacteria were found in the Vm-MBs + UTMD group than in the other groups ($p < 0.001$, independent-samples *t*-test). Similar changes were observed for *E. coli* biofilm ($p < 0.001$, independent-samples *t*-test) (Figure 4h). As shown in Figures 4e and 4i, the bacteria within the MRSA biofilms in the Vm-MBs + UTMD group showed the most significant reduction ($p = 0.31$, independent-samples *t*-test), much higher than in the UTMD group (51.35%). The bacteria within the *E. coli* biofilms in the Mp-MBs + UTMD group showed the most significant reduction ($p < 0.001$), which was much higher than that in the UTMD group (46.81%) (Figure 5a) ($p < 0.001$, both independent-samples *t*-test).

Moreover, SEM was used to investigate the morphology changes of bacteria after various treatments, indicating bacterial activity. As shown in Figure 5b, control group MRSA bacteria were typically spherical-shaped with intact and smooth cell walls, and many bacteria accumulated. With the increase in biofilm breakdown, antibiotic penetration efficiency, and antibacterial activity, the MRSA cell walls became wrinkled and rough in the UTMD and Vm-MBs + UTMD groups. The Vm-MBs + UTMD group was the most notable for this, with only a small amount of remaining bacteria. Similar morphology changes could be observed when *E. coli* bacteria was the experimental model.

Discussion

Our study is the first to explore the potential of Vm-MBs or Mp-MBs to infiltrate bacterial biofilms. Nevertheless, we used them in combination with US to assess the sonodynamic effect. The results indicate that Vm-MBs + UTMD or Mp-MBs + UTMD can significantly change the structure of biofilms and enhance the bactericidal activity of Vm or Mp.

MBs are micrometre-scale spheres with gas cores and stabilizing shells. They have been considered not only as clinical contrast agents but also as alternative platforms for drug delivery, due to their unique sonodynamic effect.[28-31] In this study, Vm-MBs or Mp-MBs were created using the thin-film hydration method,[22] maintaining high drug loading and encapsulation rates in stable conditions. The MBs were constructed with a phospholipid bilayer configuration, allowing for the accommodation of hydrophilic Vm or Mp internally, thus avoiding direct exposure to the biofilm that can lead to antibiotic deactivation. The structural integrity of Vm-MBs or Mp-MBs preserved antimicrobial efficacy and facilitated enhanced infiltration into the recalcitrant biofilm matrix. This improved penetration capability is likely due to the phospholipid bilayer's resemblance to cellular membranes, which is thought to play a role in their cellular uptake.[32] This aligns with Walsh et al's[33] findings, which showed that liposome-encapsulated antibiotics, such as AmBisome with amphotericin B integrated into the lipid bilayer, had better permeability compared to free antibiotics in antifungal use, highlighting the crucial role of liposomal bilayers in biofilm interactions.

According to EUCAST,[34] the MRSA epidemiological cut-off value (ECOFF) is 2 μg/ml. The complexity of biofilms, whether formed on prosthetic devices or biological tissues, requires antibiotic dosages that are 1,000-fold higher than those effective against planktonic counterparts. This is due to the dense and intricate 3D structure of biofilms, which acts as a barrier to antibiotic diffusion. Jefferson et al[35] previously highlighted the risk associated with the increased antibiotic dosages needed for biofilm penetration, which may lead to systemic toxicity beyond the threshold of human safety. High-resolution CLSM analysis in this study showed that most non-encapsulated antibiotics were stopped at the biofilm surface, unable to penetrate and reach lethal levels within its internal matrix. This ineffective penetration causes antibiotics to be used up by surface bacteria over time, reducing their effectiveness and potentially promoting antibiotic-resistant populations within the biofilm. The Vm-MBs or Mp-MBs prepared for this study had the potential to penetrate the deeper layers of the biofilm and enhance the effectiveness of antibiotics in reaching those deeper layers. However, although the Vm-MBs and Mp-MBs remained stable, fewer free antibiotics were available, thus allowing many live bacteria to persist within the biofilm. As a result, the antibiotic-loaded MBs must be combined with US to produce sonodynamic effects that disrupt the permeability of the tissue surrounding the MBs, and target the drug release inside the MBs.

Sonodynamic therapy is a safe physical targeting method with positive application prospects in the treatment of cancer,[36] acute cardiac transplantation rejection therapy,[22] and ocular diseases.[37] This study applied sonodynamic therapy to MRSA and *E. coli* biofilm treatment, and the results indicate that the method was strong in disrupting the biofilm structure, but was weak in killing bacteria. As sonodynamic therapy can disrupt the structural integrity of the microvesicle periphery through mechanical forces, eventual sterilization may also require the involvement of antibiotics. In the present study, UTMD was combined with Vm-MBs or Mp-MBs, and the results revealed that the removal of biofilm and killing of bacteria were statistically significantly improved. This result demonstrates that UTMD alone only disrupts biofilm structure, and that the bactericidal efficacy is greatly enhanced in combination with antibiotics. The possible reason for the results could be as follows. First, MBs protectively carry antibiotics into the deep layer of biofilms. The antibiotics penetrate the deeper layer of the biofilm along with the MBs. After the intervention with UTMD, the MBs have a cavitation effect, destroying the structure of the surrounding biofilm and releasing the antibiotics into the deeper layer accurately to improve the antibiotics' ability to exercise bactericidal activity more deeply. Second, the antibiotics' ability to kill deep bacteria was enhanced so that the number of deep bacteria decreased, the extracellular matrix produced by the bacteria (e.g. adhesins, bacterial toxins) decreased, and the biofilm further disintegrated and died. Therefore, the biofilms in the Vm-MBs +

UTMD group or Mp-MBs + UTMD group were easily eradicated during the experiment. Kouijzer et al[38] discovered that UTMD enhances the anti-biofilm and bactericidal effectiveness of Vm, however the treatment effect of the Vm + UTMD group was not investigated in this study, so it is unclear whether there is a difference in treatment effect between Vm or Mp + UTMD and Vm-MBs or Mp-MBs + UTMD. Compared with Kouijzer et al's[38] "two-steps" method, our study changed the "two steps" into "one step", which not only improves the experiment's efficiency but also refines the drug delivery method. Some scholars have suggested that, although the Vm + UTMD treatment method has a significant destructive effect on the biofilm and a certain degree of bactericidal efficacy, there are limitations in the bactericidal efficacy of the method, mainly because UTMD destroys the structure of the biofilm.[39–41] However, there is still a large amount of EPS, and adding antibiotics and EPS directly creates a chemical reaction that reduces the antibiotic activity, limiting the bactericidal efficacy of Vm or Mp + UTMD. The Vm-MBs or Mp-MBs + UTMD used in this study decreased the experimental steps and encapsulated the antibiotics inside the MBs, which exerted a cavitation effect. This released the antibiotics in a targeted manner and avoided contact between the antibiotics and the external EPS, which reduced the inactivation rate and improved the bactericidal efficacy. In the study, we found that removing and sterilizing *E. coli* biofilm after treatment using Mp-MBs + UTMD was significantly more effective than for MRSA. A previous study has shown that US statistically significantly affects Gram-negative bacteria such as *E. coli, Pseudomonas aeruginosa, Klebsiella aerogenes*, and *Salmonella,* and the biological impact of US on Gram-positive bacteria is weak.[42] The possible mechanism is the difference in Gram-positive and Gram-negative bacteria's cell wall structures and biofilms.

Our study has some limitations. First, it is noted that antibiotic penetration into biofilm is time-dependent, and there was a lack of investigation into the time-based relationship between antibiotic and drug-loaded MB penetration. Second, our study did not design a control group containing MBs without antibiotics, which could bias our experimental results. Finally, biofilms are attached to prosthetic surfaces in vivo and are exposed to various physiological environments which differ from those formed in vitro. Therefore, our findings need to be further verified through in vivo experiments.

In conclusion, our study showed that the prepared Vm-MBs or Mp-MBs not only protect the antibiotics but also promote their entry into the deeper layers of the biofilm. Also, under the mediation of UTMD, the antibiotics can be released with precision and destroy the biofilm through the cavitation effect, which enables the antibiotics to specifically kill the deep-seated bacteria and dismantle the biofilm from the inside out. This therefore provides a new and promising strategy for the treatment of biofilm-associated infection.

References

1. **Edelstein AI**, **Weiner JA**, **Cook RW**, **et al**. Intra-articular vancomycin powder eliminates methicillin-resistant S. aureus in a rat model of a contaminated intra-articular implant. *J Bone Joint Surg Am*. 2017;99-A(3):232–238.
2. **Kim PH**, **Leopold SS**. In brief: Gustilo-Anderson classification. *Clin Orthop Relat Res*. 2012;470(11):3270–3274.
3. **Köder K**, **Hardt S**, **Gellert MS**, **et al**. Outcome of spinal implant-associated infections treated with or without biofilm-active antibiotics: results from a 10-year cohort study. *Infection*. 2020;48(4):559–568.
4. **Li J**, **Cheung WH**, **Chow SK**, **Ip M**, **Leung SYS**, **Wong RMY**. Current therapeutic interventions combating biofilm-related infections in orthopaedics: a systematic review of in vivo animal studies. *Bone Joint Res*. 2022;11(10):700–714.
5. **Guo H**, **Xu C**, **Chen J**. Risk factors for periprosthetic joint infection after primary artificial hip and knee joint replacements. *J Infect Dev Ctries*. 2020;14(6):565–571.
6. **Subhadra B**, **Kim DH**, **Woo K**, **Surendran S**, **Choi CH**. Control of biofilm formation in healthcare: recent advances exploiting quorum-sensing interference strategies and multidrug efflux pump inhibitors. *Materials (Basel)*. 2018;11(9):1676.
7. **Li Y**, **Zhang X**, **Ji B**, **et al**. One-stage revision using intra-articular carbapenem infusion effectively treats chronic periprosthetic joint infection caused by Gram-negative organisms. *Bone Joint J*. 2023;105-B(3):284–293.
8. **Ji B**, **Li G**, **Zhang X**, **et al**. Effective single-stage revision using intra-articular antibiotic infusion after multiple failed surgery for periprosthetic joint infection: a mean seven years' follow-up. *Bone Joint J*. 2022;104-B(7):867–874.
9. **Karimi A**, **Karig D**, **Kumar A**, **Ardekani AM**. Interplay of physical mechanisms and biofilm processes: review of microfluidic methods. *Lab Chip*. 2015;15(1):23–42.
10. **Pai L**, **Patil S**, **Liu S**, **Wen F**. A growing battlefield in the war against biofilm-induced antimicrobial resistance: insights from reviews on antibiotic resistance. *Front Cell Infect Microbiol*. 2023;13:1327069.
11. **Hamad C**, **Chowdhry M**, **Sindeldecker D**, **Bernthal NM**, **Stoodley P**, **McPherson EJ**. Adaptive antimicrobial resistance, a description of microbial variants, and their relevance to periprosthetic joint infection. *Bone Joint J*. 2022;104-B(5):575–580.
12. **Xiu W**, **Ren L**, **Xiao H**, **et al**. Ultrasound-responsive catalytic microbubbles enhance biofilm elimination and immune activation to treat chronic lung infections. *Sci Adv*. 2023;9(4):eade5446.
13. **Knoll L**, **Steppacher SD**, **Furrer H**, **Thurnheer-Zürcher MC**, **Renz N**. High treatment failure rate in haematogenous compared to non-haematogenous periprosthetic joint infection. *Bone Joint J*. 2023;105-B(12):1294–1302.
14. **Rajput V**, **Meek RMD**, **Haddad FS**. Periprosthetic joint infection: what next? *Bone Joint J*. 2022;104-B(11):1193–1195.
15. **Teirlinck E**, **Xiong R**, **Brans T**, **et al**. Laser-induced vapour nanobubbles improve drug diffusion and efficiency in bacterial biofilms. *Nat Commun*. 2018;9(1):4518.
16. **Pijls BG**, **Sanders I**, **Kuijper EJ**, **Nelissen RGHH**. Effectiveness of mechanical cleaning, antibiotics, and induction heating on eradication of *Staphylococcus aureus* in mature biofilms. *Bone Joint Res*. 2022;11(9):629–638.
17. **Tahir W**, **Zeeshan T**, **Waseem S**, **et al**. Impact of silver substitution on the structural, magnetic, optical, and antibacterial properties of cobalt ferrite. *Sci Rep*. 2023;13(1):15730.
18. **Müller A**, **Preuß A**, **Röder B**. Photodynamic inactivation of Escherichia coli - correlation of singlet oxygen kinetics and phototoxicity. *J Photochem Photobiol B*. 2018;178:219–227.
19. **Guo H**, **Wang Z**, **Du Q**, **Li P**, **Wang Z**, **Wang A**. Stimulated phase-shift acoustic nanodroplets enhance vancomycin efficacy against methicillin-resistant *Staphylococcus aureus* biofilms. *Int J Nanomedicine*. 2017;12:4679–4690.
20. **El-Gamal MI**, **Brahim I**, **Hisham N**, **Aladdin R**, **Mohammed H**, **Bahaaeldin A**. Recent updates of carbapenem antibiotics. *Eur J Med Chem*. 2017;131:185–195.
21. **Aboltins CA**, **Berdal JE**, **Casas F**, **et al**. Hip and Knee Section, Prevention, Antimicrobials (Systemic): Proceedings of International Consensus on Orthopedic Infections. *J Arthroplasty*. 2019;34(2S):S279–S288.
22. **Liu J**, **Chen Y**, **Wang G**, **et al**. Improving acute cardiac transplantation rejection therapy using ultrasound-targeted FK506-loaded microbubbles in rats. *Biomater Sci*. 2019;7(9):3729–3740.
23. **Kot B**, **Sytykiewicz H**, **Sprawka I**, **Witeska M**. Effect of *trans*-cinnamaldehyde on methicillin-resistant *Staphylococcus aureus* biofilm formation: metabolic activity assessment and analysis of the biofilm-associated genes expression. *Int J Mol Sci*. 2019;21(1):102.
24. **Castanheira M**, **Huband MD**, **Mendes RE**, **Flamm RK**. Meropenem-vaborbactam tested against contemporary gram-negative isolates

collected worldwide during 2014, including Carbapenem-resistant, KPC-producing, multidrug-resistant, and extensively drug-resistant Enterobacteriaceae. *Antimicrob Agents Chemother*. 2017;61(9):e00567-17.
25. **Guan L**, **Wei Y**, **Dou J**, **et al**. Optimising the efficacy of targeted gene-carrying ultrasound nanobubbles: an experimental study. *China Med Imaging Technology*. 2022;38(9):1281–1285.
26. **Bjånes T**, **Kotopoulis S**, **Murvold ET**, **et al**. Ultrasound- and microbubble-assisted gemcitabine delivery to pancreatic cancer cells. *Pharmaceutics*. 2020;12(2):141.
27. **Boyte ME**, **Benkowski A**, **Pane M**, **Shehata HR**. Probiotic and postbiotic analytical methods: a perspective of available enumeration techniques. *Front Microbiol*. 2023;14:1304621.
28. **Jamburidze A**, **Huerre A**, **Baresch D**, **Poulichet V**, **De Corato M**, **Garbin V**. Nanoparticle-coated microbubbles for combined ultrasound imaging and drug delivery. *Langmuir*. 2019;35(31):10087–10096.
29. **Sun T**, **Jiang C**. Stimuli-responsive drug delivery systems triggered by intracellular or subcellular microenvironments. *Adv Drug Deliv Rev*. 2023;196:114773.
30. **Lattwein KR**, **Shekhar H**, **Kouijzer JJP**, **van Wamel WJB**, **Holland CK**, **Kooiman K**. Sonobactericide: an emerging treatment strategy for bacterial infections. *Ultrasound Med Biol*. 2020;46(2):193–215.
31. **Wang G**, **Zhang S**, **Lu H**, **Mu Y**. Therapeutic angiogenesis for ovarian transplantation through ultrasound-targeted microbubble destruction. *Ultrasound Med Biol*. 2021;47(7):1868–1880.
32. **Kooiman K**, **Roovers S**, **Langeveld SAG**, **et al**. Ultrasound-responsive cavitation nuclei for therapy and drug delivery. *Ultrasound Med Biol*. 2020;46(6):1296–1325.
33. **Walsh TJ**, **Goodman JL**, **Pappas P**, **et al**. Safety, tolerance, and pharmacokinetics of high-dose liposomal amphotericin B (AmBisome) in patients infected with Aspergillus species and other filamentous fungi: maximum tolerated dose study. *Antimicrob Agents Chemother*. 2001;45(12):3487–3496.
34. **Giske CG**, **Turnidge J**, **Cantón R**, **Kahlmeter G**, **EUCAST Steering Committee**. Update from the European Committee on Antimicrobial Susceptibility Testing (EUCAST). *J Clin Microbiol*. 2022;60(3):e0027621.
35. **Jefferson KK**, **Goldmann DA**, **Pier GB**. Use of confocal microscopy to analyze the rate of vancomycin penetration through Staphylococcus aureus biofilms. *Antimicrob Agents Chemother*. 2005;49(6):2467–2473.
36. **Wanigasekara J**, **de Carvalho AMA**, **Cullen PJ**, **Tiwari B**, **Curtin JF**. Converging technologies: targeting the hallmarks of cancer using ultrasound and microbubbles. *Trends Cancer*. 2021;7(10):886–890.
37. **Rousou C**, **Schuurmans CCL**, **Urtti A**, **et al**. Ultrasound and microbubbles for the treatment of ocular diseases: from preclinical research towards clinical application. *Pharmaceutics*. 2021;13(11):1782.
38. **Kouijzer JJP**, **Lattwein KR**, **Beekers I**, **et al**. Vancomycin-decorated microbubbles as a theranostic agent for Staphylococcus aureus biofilms. *Int J Pharm*. 2021;609:121154.
39. **Davies D**. Understanding biofilm resistance to antibacterial agents. *Nat Rev Drug Discov*. 2003;2(2):114–122.
40. **Dong Y**, **Xu Y**, **Li P**, **Wang C**, **Cao Y**, **Yu J**. Antibiofilm effect of ultrasound combined with microbubbles against Staphylococcus epidermidis biofilm. *Int J Med Microbiol*. 2017;307(6):321–328.
41. **He N**, **Hu J**, **Liu H**, **et al**. Enhancement of vancomycin activity against biofilms by using ultrasound-targeted microbubble destruction. *Antimicrob Agents Chemother*. 2011;55(11):5331–5337.
42. **Cai Y**, **Wang J**, **Liu X**, **Wang R**, **Xia L**. A review of the combination therapy of low frequency ultrasound with antibiotics. *Biomed Res Int*. 2017;2017:2317846.

Author information

L. Yao, MD, Orthopaedic Surgeon,
Department of Sports Medicine, First Affiliated Hospital of Xinjiang Medical University, Urumqi, China.

C. Chu, MD, Orthopaedic Surgeon, Department of Joint Surgery, First Affiliated Hospital of Sun Yat-sen University, Guangzhou, China.

Y. Li, MD, PhD, Orthopaedic Surgeon, Department of Orthopaedics, First Affiliated Hospital of Xinjiang Medical University, Urumqi, China.

L. Cao, MD, Orthopaedic Surgeon, Department of Orthopaedics, First Affiliated Hospital of Xinjiang Medical University, Urumqi, China; Key Laboratory of High Incidence Disease Research in Xinjiang (Xinjiang Medical University), Ministry of Education, Urumqi, China.

J. Yang, MD, Research Fellow, College of Pharmacy, Xinjiang Medical University, Urumqi, China.

W. Mu, MD, PhD, Orthopaedic Surgeon, Department of Orthopaedics, First Affiliated Hospital of Xinjiang Medical University, Urumqi, China; College of Pharmacy, Xinjiang Medical University, Urumqi, China.

Author contributions

L. Yao: Conceptualization, Data curation, Formal analysis, Methodology, Validation, Visualization, Writing – original draft, Investigation.
C. Chu: Data curation, Formal analysis, Methodology, Validation, Visualization, Writing – original draft.
Y. Li: Investigation, Validation, Visualization.
L. Cao: Funding acquisition, Investigation, Project administration, Supervision.
J. Yang: Conceptualization, Funding acquisition, Supervision.
W. Mu: Conceptualization, Funding acquisition, Project administration, Supervision, Writing – review & editing, Investigation.

L. Yao and C. Chu contributed equally to this work.

L. Yao and C. Chu are joint first authors.

Funding statement

The authors disclose receipt of the following financial or material support for the research, authorship, and/or publication of this article: this study was supported by grants from the National Natural Science Foundation of China (No.82260435), the Natural Science Foundation of Xinjiang (2021D01C331), and the Natural Science Foundation of Xinjiang Autonomous Region (2023D01E11).

ICMJE COI statement

All authors report grants from the National Natural Science Foundation of China (No.82260435), the Natural Science Foundation of Xinjiang (2021D01C331), and the Natural Science Foundation of Xinjiang Autonomous Region (2023D01E11), related to this study. The authors have no other relevant financial or non-financial interests to disclose, and the final manuscript has been approved by all authors for publication.

Data sharing

The datasets generated and analyzed in the current study are not publicly available due to data protection regulations. Access to data is limited to the researchers who have obtained permission for data processing. Further inquiries can be made to the corresponding author.

Acknowledgements

The authors thank Zhibiao Dong for his technical assistance in designing the figures.

Open access funding

The authors report that they received open access funding for their manuscript from the National Natural Science Foundation of China (No.82260435), the Natural Science Foundation of Xinjiang (2021D01C331), and the Natural Science Foundation of Xinjiang Autonomous Region (2023D01E11).